IEEE Access
Multidisciplinary | Rapid Review | Open Access Journal

Received January 14, 2018, accepted February 21, 2018, date of publication March 1, 2018, date of current version March 28, 2018.

Digital Object Identifier 10.1109/ACCESS.2018.2810941

Speed Synchronization Control for Integrated Automotive Motor-Transmission Powertrains Over CAN Through a Co-Design Methodology

WANKE CAO[1], YINGSHUANG WU[1], YUHUA CHANG[2], ZHIYIN LIU[2], CHENG LIN[1], QIANG SONG[1], AND ANTONI SZUMANOWSKI[2]

[1]National Engineering Laboratory for Electric Vehicles and Collaborative Innovation Center of Electric Vehicles in Beijing, School of Mechanical Engineering, Beijing Institute of Technology, Beijing 100081, China
[2]Department of Multisource Propulsion system, Faculty of Automotive and Construction Machinery Engineering, Warsaw University of Technology, 02-524 Warsaw, Poland

Corresponding authors: Wanke Cao (caowanke@bit.edu.cn)

This work was supported in part by the National Natural Science Foundation of China under Grant 51575044 and in part by the National Key Research and Development Program of China under Grant 2017YFB0103801.

ABSTRACT This paper deals with the speed synchronization controller design for networked integrated motor-transmission (IMT) powertrains via controller area network (CAN). It is well known that, in current implementations, CAN has been widely used in the control system design of automotive powertrains. However, on the other hand, the application of CAN would not only lead to network-induced delays but also bring about protocol constrains, e.g., data package capability and utilization ratio limitation, which would deteriorate the system and make the controller design a challenging problem. This paper is to provide a co-design methodology that can cope with all these problems and ensure satisfactory control effect for the speed synchronization control of IMT powertrain systems. First, a networked IMT powertrain system using CAN as underlying network is presented and the dynamic model for the speed synchronization control is derived. Second, the network-induced delay model is introduced and improved considering data packet capability and utilization ratio limitation. The control-orient discrete-time model is also derived based on the improved delay model. Third, a co-design methodology using sliding mode controller and offline priority scheduling based on Lyapunov stability criterion is proposed. The results of simulations and tests show the effectiveness of the proposed co-design methodology.

INDEX TERMS Integrated motor-transmission (IMT), speed synchronization control, sliding mode control, network-induced delay, protocol constrain, co-design of scheduling and control.

I. INTRODUCTION

Integrated motor-transmission (IMT) powertrains are considered to be good choices for electric vehicles (EVs) because of their advantages in terms of vehicle drivability improvement, energy optimization and reducing the motor size [1]–[6]. According to recent researches [1]–[5], with the electric motor's fast and precise response, the shifting process can be executed by the coordination control between driving motor and transmission based on the active motor speed and torque control. Therefore, the clutch is no longer necessary for the IMT powertrains [5], [7]–[12]. In other words, the driving motor and transmission can be directly coupling, which can further simplify the powertrain system's structure a lot. Thus, there have been various researches on the clutchless IMT powertrain for EVs [7], [13]–[16]. Moreover, for automotive powertrains, different transmissions have been developed and applied, e.g., automatic transmission (AT), continuously variable transmission (CVT), dual clutch transmission (DCT) and automated manual transmission (AMT), etc [8]. Owing to higher transmission efficiency and lower cost, AMT has been widely adopted in the IMT powertrain design for EVs [7], [9]–[11].

While enjoying the advantages of structure simplification, the control system design for the clutchless IMT powertrain becomes a challenging problem. According to the research of Tseng and Yu [7], for a clutchless IMT powertrain based on AMT, the shifting process usually consists of seven phases as follows: 1) releasing the motor torque; 2) shifting to

neutral position; 3) selecting the target gear; 4) adjusting the motor speed (electronic synchronization control); 5) releasing the motor torque; 6) engaging (mechanical synchronization); 7) restoring the motor speed (a strategy on the shifting process control for clutchless IMT powertrains in details, see [7]). The electronic synchronization is an additional requirement in the shifting process due to the absence of clutch, which aims to guarantee the synchronization between the motor and transmission in the shifting process. Some researchers [2], [3], [7], [21] have pointed out that the electronic speed synchronization control plays a critical role in the shifting process of clutchless IMT powertrains, which can greatly influence the shifting quality, e.g., shifting impact, shifting time and torque hole, and takes nearly half of the entire shifting time.

To improve the speed synchronization control for the clutchless IMT powertrains, the sliding mode controller (SMC), which is very robust to parameter variations and external disturbances, has been widely adopted in the controller design [7], [8], [17]. However, as a variable structure control technology, the SMC easily leads to oscillation problem due to the effects of control system, e.g., delays in control loop. Furthermore, in current implementations, the controller area network (CAN) has been widely used in the control system design for the powertrains of EVs [17]–[19]. An IMT powertrain has become a typical networked control system (NCS), where the data are exchanged via CAN from sensors to controllers and from controllers to actuators. The application of CAN would not only lead to network-induced delays but also bring out protocol constraints, e.g., data packet capability and utilization ratio limitation. These problems would deteriorate the system and make the controller design a challenge. According to the research of Caruntu *et al.* [20], CAN-induced delays led to the traditional vehicle powertrain oscillation. Zhu *et al*. [21] pointed out that CAN-induced delays led to the IMT powertrain oscillation for EVs, and proposed a robust speed synchronization control design method [8]. In our previous study [17], the oscillation phenomenon was also observed in the speed synchronization control for the IMT powertrains due to the CAN-induced delays, and an active period-scheduling approach has been presented to improve the system synchronization.

However, all these aforementioned researches for the automotive IMT powertrain control over CAN mainly focus on the network-induced delays without considering protocol constrains such as the data packet capability and utilization ratio limitation. In other words, the IMT powertrain over CAN is consumed as an ideal delay-time system. From the perspective of networked control, it is still possible to fail for the controllers which are robust to the delays. For a NCS, the co-design of scheduling and control [22]–[25], where the control performance and protocol constrains are simultaneously considered, has great advantages, which has been widely applied in industrial networked control applications [24]–[26]. As a typical NCS, in the speed synchronization controller design for the IMT powertrains, the protocol constrains also should been considered.

Motivated by the shortcomings of existing control system design methods for the speed synchronization control, the contributions of this paper are as follows: firstly, in the system modeling process, both the network-induced delays and protocol constrains of CAN are considered. Secondly, a co-design methodology of scheduling and control is presented to deal with all the challenges and ensure the stability of speed synchronization control.

The rest part of this paper is organized as follows: In section II, the problem formulation on the speed synchronization control for a clutchless IMT powertrain system using CAN as underlying network is presented. The speed synchronization control model and the CAN-induced delays considering protocol constraints are derived. In section III, a co-design method of scheduling and control for the speed synchronization control is proposed. Moreover, from the application point of view, a discrete-time SMC is designed to improve the transient performance of the speed synchronization. Co-simulations in Simulink and CarSim are carried out to evaluate the effectiveness of the proposed controller in section IV. In section V, hardware-in-loop (HIL) tests are implemented to validate the proposed method in a real CAN environment. Finally, conclusions are summarized in section VI.

II. PROBLEM FORMULATION

In the design of clutchless IMT powertrains, AMT has been widely used because of its advantages such as light weight, low cost and high efficiency. In this study, a clutchless IMT powertrain system is considered, where a driving motor and a two-speed AMT are directly coupled without clutch shown in Figure 1. In the control system, CAN is used as the communication medium to connect different electronic control units (ECUs) such as motor control unit (MCU), transmission control unit (TCU) and vehicle control unit (VCU), etc. In the shifting process, TCU controls the driving motor with MCU to work under different modes including free mode, torque mode and speed mode. The whole shifting process of the clutchless IMT system in detail can be referred to in [7] and [27].

As a key issue in the clutchless shifting process, the speed synchronization control can be realized through active control of the motor with the speed measurements from sensors, e.g., the motor speed sensor and the transmission speed sensor. Usually, the motor speed sensor is connected to MCU and the transmission speed sensor is connected to TCU. The control command is computed by TCU. The measurements and control signals are exchanged via CAN, which makes the IMT system a typical NCS as shown in Figure 2.

A. DYNAMICS MODEL OF IMT SYSTEM

A typical simplified dynamics structure as shown in Figure 3, which is widely used in the control system design for the IMT powertrains [20], is adopted in this study.

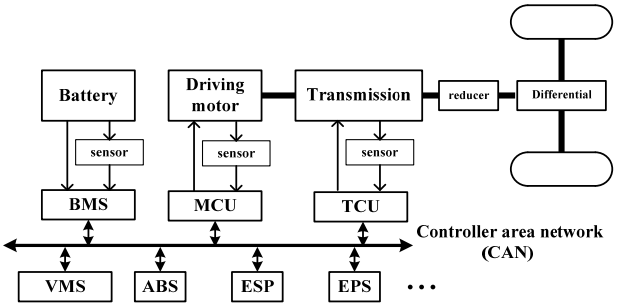

FIGURE 1. Integrated motor-transmission powertrain system diagram over CAN.

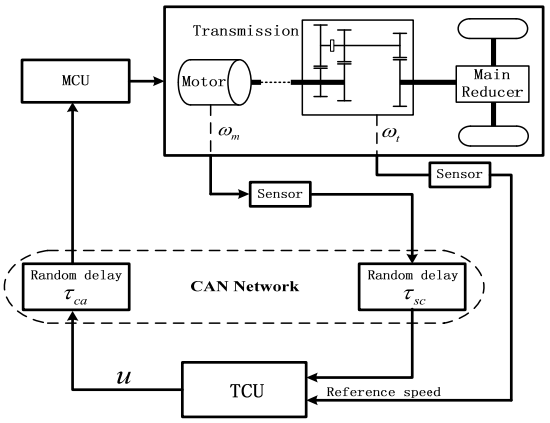

FIGURE 2. Networked control system for the speed synchronization control.

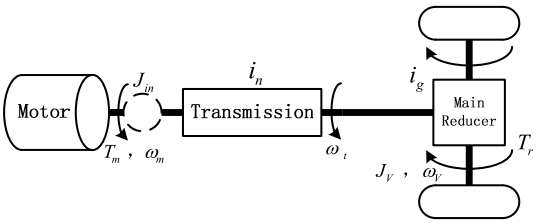

FIGURE 3. Simplified dynamics model of clutchless IMT system.

According to Zhu *et al.* [8], during the speed synchronization phase, the dynamic equations of the powertrain system can be written as:

$$\begin{cases} J_{in}\dot{\omega}_m = T_m \\ \omega_t = \omega_V \cdot i_g \\ J_V\dot{\omega}_V = -T_r = -\left(Mg\sin(\theta r) + fMgr + \frac{1}{2}\rho_{air}AC_DV^2r_r\right) \end{cases} \tag{1}$$

where J_{in} is driving motor's equivalent inertia converted to input shaft of transmission, ω_m is rotational speed of driving motor, T_m is electric motor torque, ω_t is rotational speed of transmission, ω_V is rotational speed of wheel, i_g is main reducer ratio, J_V is equivalent inertia of vehicle simplified to wheel shaft, T_r is road gradient resistant torque of vehicle, M is total mass of vehicle, θ is slope angle of road, r is radius of tire, f is rolling resistance coefficient, ρ_{air} is air density, A is front area of the vehicle, C_D is coefficient of aerodynamic drag toque, V is vehicle speed.

A brushless direct current motor (BLDCM) is adopted as the driving motor in this study as in [7]. Without losing generality, the simplified dynamics model of the motor-driving system can be expressed as below [8], [10]:

$$\dot{\omega}_m = a\omega_m + bu \tag{2}$$

where a and b are undetermined parameters, u is control input voltage of MCU.

According to Tseng and Yu [7], the method named recursive least square (RLS) algorithm can be used to identify the undetermined parameters a and b of the motor-driving system based on measuring the motor speed and the control input voltage (The identification of parameters, see [9]).

For the obtained model of the motor-driving system, while assuming the system works in time-driven mode with a fixed sampling period T without considering the system delays, the discrete-time model of the motor-driving system can be described as follows:

$$\omega_{k+1} = a_d\omega_k + b_du_k \tag{3}$$

where

$$a_d = e^{aT}, \quad b_d = \int_0^T e^{as}ds \cdot b$$

B. SPEED SYNCHRONIZATION CONTROL PURPOSE ANALYSIS

As mentioned above, the purpose of speed synchronization control is to guarantee the synchronization between the motor and the transmission by actively regulating the motor speed. From the view of rotational kinematics of an IMT system, as shown in Figure 3, the connection between the motor and the transmission is assumed to be rigid, therefore the synchronization between the motor and the transmission can be described quantitatively as an expression: $\omega_m = \omega_t \cdot i_n$, where ω_m denotes the motor speed, ω_t denotes the transmission speed and i_n denotes the current transmission ratio. In the IMT system, different gear pair usually leads to different transmission ratio. In a shifting process such as from i_n to i_{n+1}, the target motor speed can be described as $\omega_{m_t} = \omega_T \cdot i_{n+1}$, where i_{n+1} denotes the target transmission ratio. Correspondingly, the speed difference between the current motor speed and the target motor speed is the necessary motor speed adjustment for rapid and smooth shifting gears as follows [8]:

$$\Delta\omega = \omega_{\text{target}} - \omega_{motor} = \frac{v}{r}(i_{n+1} - i_n)i_g \tag{4}$$

In the upshifting process, as $i_{n+1} < i_n$, the motor speed is required to reduce by $|\Delta\omega_m|$. Conversely, in downshifting process, $i_{n+1} > i_n$, the motor speed should increase by $|\Delta\omega_m|$.

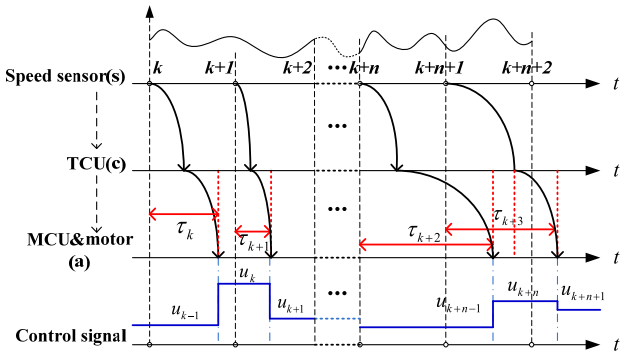

FIGURE 4. Network-induced delay map.

C. NETWORK-INDUCED DELAY ANALYSIS

As shown in Figure 2, CAN is used in both feedback and forward channels for the control system, so the network-induced delays will be inevitably imposed into the control loop as shown in Figure 4. And the entire network-induced delays in the loop can be described as follows:

$$\tau_k = \tau_{\mathrm{ca},k} + \tau_{\mathrm{sc},k}, \quad k = 0, 1, 2, \ldots \tag{5}$$

where τ_k is the entire network-induced delay in the loop at kth period, $\tau_{ca,k}$ is network-induced delay in forward link at kth period, $\tau_{sc,k}$ is network-induced delay in feedback link at kth period.

In the shifting process, it is necessary to ensure rapid response of the control system. Therefore, it is reasonable to assume that: the sensor node works in time-driven mode with the fixed sample period; both the controller node and the actuator node work in event-driven mode, in which the nodes will immediately implement a specified task once a valid packet is received via CAN, and the task execution time in each node can be ignored.

With such assumptions, the network-induced delays in loop of the IMT control system are shown in Figure4. And the upper bound of the CAN-induced delays of each packet can be determined through an expression considering the data packet capability and utilization ratio limitation, which is described as follows [29], [30]:

$$R_{worst,j} = t_j + C_j - 3\tau_{bit}, \quad j \in \{1, 2, \ldots N\} \tag{6}$$

where

$$t_j^{n+1} = B_j + \sum_{i=1}^{j-1} \left\lceil \frac{t_j^n + \tau_{bit}}{T_i} \right\rceil C_i \tag{7}$$

$$C_j = \left(\left\lfloor \frac{53 + 8d_j}{4} \right\rfloor + 67 + 8d_j \right) / f_{baud}, \quad d_j \le 8 \tag{8}$$

$$N \in \{N \in Z_+ | U_{net} = \sum_{i=1}^{N} \frac{C_i}{T_i} \le 100\%\} \tag{9}$$

with $R_{worst,j}$ being the worst-case response time of the message j passing through network, which consists of the queuing delay and physical transmission time; t_j being the worst-case queuing delay of the message j, which can be calculated by a recursion formula in (7); C_j being the maximum physical transmission time of the message j with frame interval of 3 bits considering the data package capability; τ_{bit} being the time taken to transmit a bit on CAN; B_j being the maximum blocked time for the message j, equaling the maximum physical transmission time of any lower-priority message being transmitted which can be calculated by the expression in (8); f_{baud} being the network baud rate; N being the number of messages, which also denotes the upper bound of priority j and subject to the network utilization ratio limitation as in (9); U_{net} being the network utilization rate, which can be calculated as in the expression (9); Z_+denoting positive integer set; T_i being the period of the message j; d_j being the data length in a packet subject to the protocol of CAN; j being the ID tag of the message j, which also denotes the priority of the message j, and in a CAN-based system the smaller the value of the j, the greater the priority.

According to Figure 2 and expression (5), the network-induced delays in the loop can be described as

$$\begin{cases} \tau_{ca,k} \le R_{worst,j_{ca}} \\ \tau_{sc,k} \le R_{worst,j_{sc}} \\ \tau_k \le R_{worst,j_{ca}} + R_{worst,j_{sc}} = \tau_{\max} \end{cases} \tag{10}$$

where, j_{ca} denotes the message in forward link of the loop, j_{sc} denotes the message in feedback link of the loop, $R_{worst,j_{ca}}$ denotes the worst-case response time of the message j_{ca}, $R_{worst,j_{sc}}$ denotes the worst-case response time of the message j_{sc}, $\tau_{\max,ca}$ denotes the maximum delay in forward link, $\tau_{\max,sc}$ denotes the maximum delay in feedback link, $\tau_{\max}$ denotes the maximum delay in the loop.

Moreover, from the real-time control point of view, it is necessary to ensure that measurement/control packets are not loss and the latest measurement or control signal is used in the shifting control process. Therefore, according to Figure 4, it is reasonable to assume that the time-varying network-induced delays should satisfy the expressions as follows:

$$\tau_{sc} < T \tag{11}$$

$$\tau_{sc} + \tau_{ca} = \tau < \tau_{sc} + T < 2T \tag{12}$$

D. CONTROL-ORIENT DISCRETE-TIME MODELS WITH RANDOM DELAYS

As shown in Figure 4, due to the network-induced delays caused by CAN, the dynamics model of the system with the delayed input can be described as

$$\begin{cases} \dot{\omega}(t) = a\omega(t) + bu(t) \\ u(t) = u_k, t \in [kT + \tau_k, (k+1)T + \tau_{k+1}] \end{cases} \tag{13}$$

Generally, in the case of lower network utilization ratio, e.g., the network-induced delays in the loop satisfy $\tau_{\max} < T$, the dynamics model of the system can be described as follows:

$$\omega_{k+1} = a_d\omega_k + \Gamma_1 u_k + \Gamma_2 u_{k-1} \tag{14}$$

where $\Gamma_1 = \int_0^{T-\tau_k} e^{as} ds \cdot b$, $\Gamma_2 = \int_{T-\tau_k}^{T} e^{as} ds \cdot b$

Whereas, in the case of higher network utilization ratio, e.g., the network-induced delays in the loop satisfy $T \leq \tau_{\max} < 2T$, the second dynamics model of the system can be described as follows:

$$\omega_{k+1} = a_d\omega_k + \Gamma_3 u_{k-1} + \Gamma_4 u_{k-2} \tag{15}$$

where $\Gamma_3 = \int_0^{2T-\tau_{k-1}} e^{as}ds \cdot b$, $\Gamma_4 = \int_{2T-\tau_{k-1}}^{T} e^{as}ds \cdot b$

III. CO-DESIGN METHOD

To ensure the stability of speed synchronization, a co-design methodology will be presented to deal with the effects of network-induced delays while considering the protocol constraints in this section, which is based on Lyapunov stability criterion and offline priority scheduling. Moreover, as mentioned above, from the application point of view, a discrete-time SMC is also designed to improve the transient performance of the speed synchronization control.

A. DISCRETE-TIME SLIDING MODE CONTROLLER DESIGN

As mentioned above, the speed synchronization control of the IMT system can be described as the speed tracking control of the driving motor. To improve the transient performance of the speed tracking, a discrete-time SMC is designed.

Firstly, to ensure the accuracy of the motor speed tracking, a sliding mode surface function is defined as follows

$$S(\omega) = e = \omega_{m,r} - \omega_m \tag{16}$$

where $\omega_{m,r}$ is the reference motor speed.

To ensure the rapid response of the motor speed tracking and dealing with the chattering problem, a discrete-time reaching law with the boundary layer of a saturation function is defined as follows

$$\frac{S_{k+1} - S_k}{T} = -Ksat(\frac{S_k}{H}),\ K > 0 \tag{17}$$

where

$$sat\left(\frac{s}{H}\right) = \begin{cases} +1 & if\ \ \text{s>H} \\ \dfrac{s}{H} & if\ |s| < H \\ -1 & if\ s < -H \end{cases}$$

Then, for the discrete-time motor-driving system as in (3), a discrete-time control law with the parameter H can be derived as follows

$$u_k = \frac{1-a_d}{b_d}\omega_{m,k} + \frac{KT}{b_d}sat(\frac{r-\omega m_{m,k}}{H}) \tag{18}$$

To ensure the reachability of the sliding mode surface, a Lyapunov function is defined as

$$V_k = S_k^2 \tag{19}$$

Theorem 1: According to Lyapunov stability criterion, for the discrete-time SMC, the sliding mode surface will be asymptotically reachable, if the following expressions can be satisfied.

$$\begin{cases} \Delta V_k = S_{k+1}^2 - S_k^2 < 0 \\ S_k \neq 0 \end{cases} \tag{20}$$

With the reaching law (17), the expression (20) can be rewritten as

$$\begin{aligned} S_{k+1}^2 - S_k^2 &= \left[S_k - KTsat(\frac{S_k}{H})\right]^2 - S_k^2 \\ &= \text{KT}\left[-2S_k sat(\frac{S_k}{H}) + KTsat^2(\frac{S_k}{H})\right] \\ &= \begin{cases} KT(-2\,|S_k| + KT), & \text{if } |S_k| > H \\ KT\left[-2\dfrac{S_k^2}{H} + KT\dfrac{S_k^2}{H^2}\right], & \text{if } |S_k| \leq H \end{cases} \end{aligned} \tag{21}$$

According to **Theorem 1**, the sliding mode surface will be asymptotically reachable, if the boundary layer parameter H can satisfy the following condition.

$$H > \frac{KT}{2} \tag{22}$$

Substituting (22) to (21), we can obtain $S_{k+1}^2 - S_k^2 < 0$.

Therefore, the discrete-time SMC with boundary layer can be designed as

$$u_k = \frac{1-a_d}{b_d}\omega_k + \frac{KT}{b_d}sat(\frac{r-\omega_k}{H}),\quad K > 0,\ H > KT/2 \tag{23}$$

B. CO-DESIGN METHOD OF SCHEDULING AND CONTROL

As mentioned above, due to the effect of CAN-induced delays, the discrete-time model of the system can be rewritten as model sets with delay pieces as in (14) and (15).

By substituting (23) into (14) and (15) respectively, we can obtain the system model sets of the networked close-loop speed synchronization control system as follows

If $\tau_{\max} < T$, substitute (23) into (14), the model set of the networked close-loop system can be written as

$$\begin{aligned} \omega_{k+1} = a_d\omega_k &+ \Gamma_1\left[\frac{1-a_d}{b_d}\omega_k + \frac{KT}{b_d}sat(\frac{r-\omega_k}{H})\right] \\ &+ \Gamma_2\left[\frac{1-a_d}{b_d}\omega_{k-1} + \frac{KT}{b_d}sat(\frac{r-\omega_{k-1}}{H})\right] \end{aligned} \tag{24}$$

Defining a new vector $Z_k = \left[\omega_{m,k}\ \omega_{m,k-1}\right]^T$, the augmented model set can be described as

$$Z_{k+1} = \phi_{ki} \cdot Z_k + W,\quad i = \{1, 2, \ldots 4\} \tag{25}$$

where

$$\phi_{k1} = \begin{bmatrix} a_d + \Gamma_1(\dfrac{1-a_d}{b_d} - \dfrac{KT}{b_d H}) & \Gamma_2(\dfrac{1-a_d}{b_d} - \dfrac{KT}{b_d H}) \\ I & 0 \end{bmatrix}$$

$$\phi_{k2} = \begin{bmatrix} a_d + \Gamma_1(\dfrac{1-a_d}{b_d}) & \Gamma_2(\dfrac{1-a_d}{b_d} - \dfrac{KT}{b_d H}) \\ I & 0 \end{bmatrix}$$

$$\phi_{k3} = \begin{bmatrix} a_d + \Gamma_1(\frac{1-a_d}{b_d} - \frac{KT}{b_d H}) & \Gamma_2(\frac{1-a_d}{b_d}) \\ I & 0 \end{bmatrix}$$

$$\phi_{k4} = \begin{bmatrix} a_d + \Gamma_1(\frac{1-a_d}{b_d}) & \Gamma_2(\frac{1-a_d}{b_d}) \\ I & 0 \end{bmatrix}$$

W denotes constant terms.

If $T < \tau_{\max} < 2T$, substitute (23) into (15), we can obtain the second model set of the networked close-loop system as follows

$$\omega_{k+1} = a_d\omega_k + \Gamma_3\left[\frac{1-a_d}{b_d}\omega_{k-1} + \frac{KT}{b_d}sat(\frac{r-\omega_{k-1}}{H})\right] + \Gamma_4\left[\frac{1-a_d}{b_d}\omega_{k-2} + \frac{KT}{b_d}sat(\frac{r-\omega_{k-2}}{H})\right] \quad (26)$$

Defining another new vector $Z'_k = \left[\omega_{m,k}\ \omega_{m,k-1}\ \omega_{m,k-2}\right]^T$, the second augmented model set can be described as

$$Z'_{k+1} = \phi'_{ki} \cdot Z'_k + W' \quad (27)$$

where

$$\phi'_{k1} = \begin{bmatrix} a_d & \Gamma_3(\frac{1-a_d}{b_d} - \frac{KT}{b_d H}) & \Gamma_4(\frac{1-a_d}{b_d} - \frac{KT}{b_d H}) \\ I & 0 & 0 \\ 0 & I & 0 \end{bmatrix}$$

$$\phi'_{k2} = \begin{bmatrix} a_d & \Gamma_3(\frac{1-a_d}{b_d}) & \Gamma_4(\frac{1-a_d}{b_d} - \frac{KT}{b_d H}) \\ I & 0 & 0 \\ 0 & I & 0 \end{bmatrix}$$

$$\phi'_{k3} = \begin{bmatrix} a_d & \Gamma_3(\frac{1-a_d}{b_d} - \frac{KT}{b_d H}) & \Gamma_4(\frac{1-a_d}{b_d}) \\ I & 0 & 0 \\ 0 & I & 0 \end{bmatrix}$$

$$\phi'_{k4} = \begin{bmatrix} a_d & \Gamma_3(\frac{1-a_d}{b_d}) & \Gamma_4(\frac{1-a_d}{b_d}) \\ I & 0 & 0 \\ 0 & I & 0 \end{bmatrix}$$

W′ denotes constant terms.

Theorem 2: According to Lyapunov stability criterion, a discrete-time system such as one in (25) is asymptotically stable if all of the eigenvalues of the system matrix set, e.g., $\phi_{ki}, \forall i \in \{1, 2, 3, 4\}$, locate within the unit circle on the complex plane as in Figure 5.

Theorem 3: According to Lyapunov stability criterion, for a unstable discrete-time system such as one in (27) with any number of eigenvalues located outside the unit circle on complex plane as in Figure 6, the discrete-time system can be stabilized if a control or scheduling approach exits, which can ensure that all of the eigenvalues of the system matrix set, e.g., $\phi'_{ki}, \forall i \in \{1, 2, 3, 4\}$, be located within the unit circle on the complex plane.

As shown in Figure 5 and Figure6, the eigenvalue locus of the system matrix sets will be gradually away from the center as the maximum delay $\tau_{\max}$ increases.

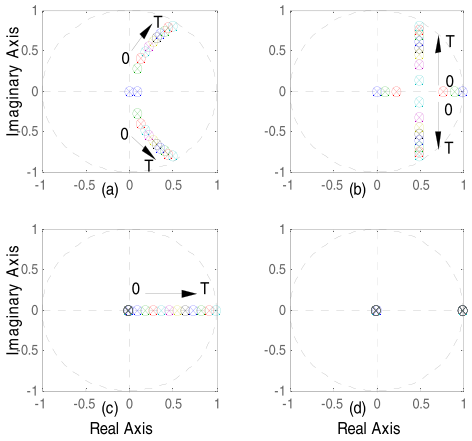

FIGURE 5. (a) The eigenvalue locus of ϕ_{k1}. (b) The eigenvalue locus of ϕ_{k2}. (c) The eigenvalue locus of ϕ_{k3}. (d) The eigenvalue locus of ϕ_{k4}.

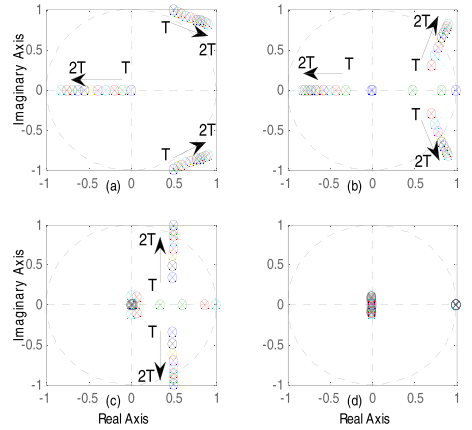

FIGURE 6. (a) The eigenvalue locus of ϕ'_{k1}. (b) The eigenvalue locus of ϕ'_{k2}. (c) The eigenvalue locus of ϕ'_{k3}. (d) The eigenvalue locus of ϕ'_{k4}.

Remark 1: According to Theorem 2, the upper bound of the maximum delay $\tau_{\max}$ can be determined when the eigenvalue locus of the system matrix sets intersects the unit circle on the complex plane, which is described as $\bar{\tau}_{\max}$. To ensure the stability of the networked close-loop system, the maximum delay in the loop should satisfy the expression as follows

$$\tau_{\max} < \bar{\tau}_{\max} \quad (28)$$

Remark 2: Combining expressions (10-12) and (28), to ensure the real-time control ability and asymptotical stability of the networked close-loop system, the network-induced delays should satisfy the expressions as follows

$$\begin{cases} \tau_{\max,sc} < T \\ \tau_{\max} < \min\{T + \tau_{\max,sc}, \bar{\tau}_{\max}\} \end{cases} \quad (29)$$

Remark 3: To design the networked close-loop system, a communication protocol file on properties of all signals, messages and network should be defined in advance. Assuming that the communication protocol file is known, to ensure that the networked close-loop system can work, the data length

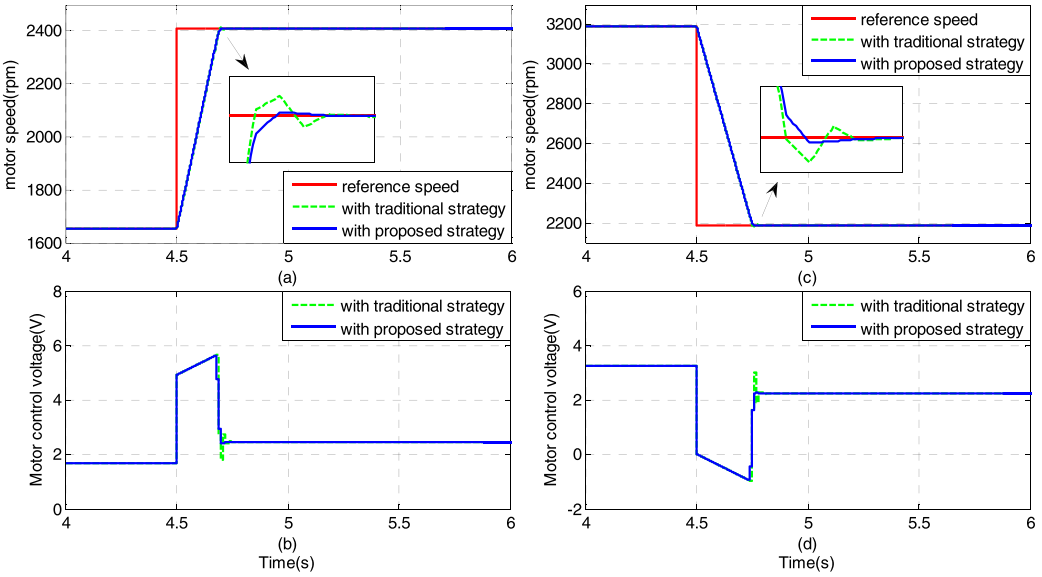

FIGURE 7. Simulation results under the ideal condition without network induced delay. (a-b) The speed synchronization in the downshift process. (c-d) The speed synchronization in the upshift process.

of each signal in the loop of the system should satisfy the expressions (8), and the message priorities j_{sc} and j_{ca} should satisfy the expressions (9). Furthermore, according to the expressions (6)-(8), the parameters of $\tau_{\max}$ and $\tau_{\max,sc}$ can be determined. If the parameters of $\tau_{\max}$ and $\tau_{\max,sc}$ satisfy the expression (29), the real-time closed-loop system will be asymptotically stable.

Remark 4: Conversely, if the parameters of $\tau_{\max}$ and $\tau_{\max,sc}$ cannot satisfy the expression (29), according to Theorem 3 and Remark 2, the closed-loop system can be stabilized if the parameters of $\tau_{\max}$ and $\tau_{\max,sc}$ can be changed to satisfy the expression (29).

Remark 5: In order to ensure that the parameters of $\tau_{\max}$ and $\tau_{\max,sc}$ satisfy the expression (29), according to the expressions (6)-(10), the lower bounds of the priorities j_{sc} and j_{ca} of messages can be determined as follows

$$\overleftarrow{j}_{sc}, \overleftarrow{j}_{ca} = \max\left(\left\{ j_{sc}, j_{ca} \;\middle|\; \begin{cases} R_{worst,j_{sc}} < T, \\ R_{worst,j_{ca}} + R_{worst,j_{sc}} \\ \qquad < \min(T + R_{worst,j_{sc}}, \bar{\tau}_{\max}) \end{cases} \right\}\right) \tag{30}$$

where $\overleftarrow{j}_{sc}$ $\overleftarrow{j}_{ca}$ are the lower bounds of the priorities j_{sc} and j_{ca}, respectively.

Remark 6: An offline priority scheduling scheme is introduced: If the message priorities $j_{sc} > \overleftarrow{j}_{sc}$ or $j_{ca} > \overleftarrow{j}_{ca}$, the message priorities j_{sc} and j_{ca} will be offline scheduled in the networked control system design phase to satisfy the expression (31) as follows

$$0 \le j_{sc} \le \overleftarrow{j}_{sc} \& 0 \le j_{ca} \le \overleftarrow{j}_{ca} j_{sc} \ne j_{ca} \tag{31}$$

IV. SIMULATION FOR SPEED SYNCHRONIZATION CONTROL

To evaluate the effectiveness of the proposed method, co-simulations are carried out in Matlab/Simulink® with a high-fidelity full vehicle model constructed by CarSim®. The parameters of the two-speed IMT powertrain are listed in Table 1, which are based on an actual prototype two-speed AMT system. The other parameters of the vehicle are based on a bench model of a C-class hatchback in CarSim® dataset.

Based on the studies in [7]–[9], the sample period of control system for the speed synchronization control is set as T = 0.01s. The fix-step is selected for the solver in Simulink as 0.001s.

Two shifting processes are selected in the co-simulations: the upshifting process and the downshifting process (see Figure 7). Considering the entire shifting process is not the focus of this study, only the speed synchronization control process is analyzed concretely in this paper.

The motor-driving system parameters of the BLDC are identified by the RLS algorithm method implemented in MATLAB as in [7] and [8]. The parameters of model (2) can be fi as:

$$\hat{a} = -1.2637 \quad \hat{b} = 1235.7$$

To ensure the rapid-response speed tracking performance without chattering phenomenon, the control gains and the boundary layer of the proposed discrete-time SMC controller are set as:

$$K = 4000 \quad H = 40$$

For the comparison purpose, a traditional SMC without considering the effects of the CAN system is also adopted

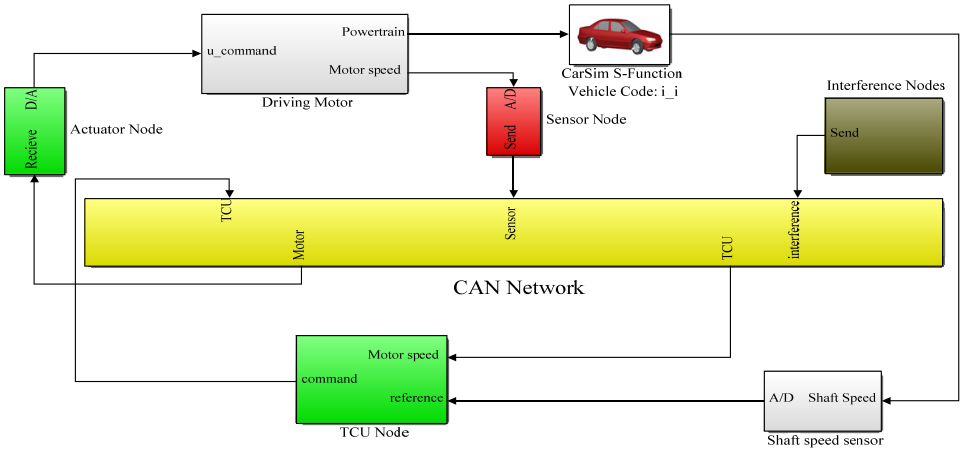

FIGURE 8. IMT powertrain system diagram with TrueTime network.

as in [9] as follows:

$$\begin{cases} e(t) = \omega_{m,r} - \omega_m(t) \\ S = e(t) \\ u_{smc} = \hat{b}^{-1}\left[\dot{\omega}_t - a\omega + \left(|(\beta-1)\dot{\omega}_t| + \left|(1-\beta)\hat{a}\omega\right|\right.\right. \\ \qquad \left.\left. + \beta F + \beta\eta\right) sat(\frac{S}{H})\right] \end{cases} \tag{32}$$

where parameters are supposed to be bounded and some variables are defined as:

$$\begin{cases} \beta = \dfrac{b_{\max}}{b_{\min}} \Rightarrow \beta \geq b\hat{b}^{-1} \geq \dfrac{1}{\beta} \\ F \geq \left|\hat{a}\omega - a_{\min}\omega\right|, \eta \geq 0 \end{cases} \tag{33}$$

Simulation results and analysis are presented in the following sections. For each shifting process, the proposed method is evaluated in two stages: the first stage is under the ideal condition without considering the effects of the CAN to evaluate the effectiveness of the designed controller; then a high-fidelity CAN model from the TrueTime toolbox is imposed into the control loop to assess the robustness of the proposed method.

A. SIMULATION UNDER IDEAL CONDITION

Figure 7 shows the simulation results of speed synchronization response under ideal condition. As shown in Figure7(a) and (c), with the proposed controller, the response time of the speed tracking control is 0.26s in downshift process and 0.30s in upshift process, respectively. Whereas, with the traditional controller, the response time of the speed tracking control is 0.28s in downshift process and 0.32s in upshift process, respectively. The results show that both the proposed controller and the traditional controller can yield satisfactory results of speed synchronization not only in the upshift process but also in the downshift process under ideal condition. Moreover, as shown in Figure7(b)(d), the simulation results show that both of the two controllers don't cause chattering of the motor control voltage signal in the speed synchronization control process.

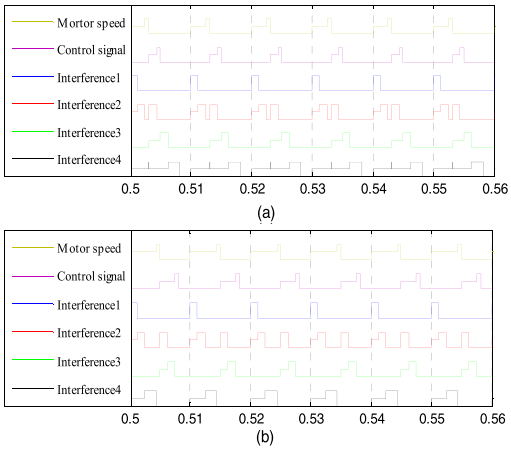

FIGURE 9. Network transmission status of the network-induced delays. (a) with the proposed method. (b) with traditional method.

B. SIMULATION WITH THE NETWORK MODEL

To assess the robustness of the proposed method against the effects of the CAN system, co-simulations with a high-fidelity CAN model are implemented by TrueTime toolbox, which is a high-fidelity Matlab-based network simulator and has been widely applied in industrial networked control system tests.

Firstly, a simplified communication protocol definition as in Table 2 is adopted, which is a 'benchmark' application to be use to evaluation different IMT control system provided by BAIC Group® where the data size of each packet is set as 8 bytes, the baud rate of CAN is set as 250kbps, 6 network nodes and 13 messages are defined respectively. Then, with the proposed controller, according to the procedure of co-design method aforementioned, we can obtain the upper delay bound $\bar{\tau}_{\max} = 7.50ms$. Moreover, according to the expressions (6)-(8), the maximum delay $\tau_{\max}$ before scheduling can be calculated as 8.308 *ms*, and the maximum delay $\tau_{\max}$ after scheduling can be calculated as 5.108 *ms*.

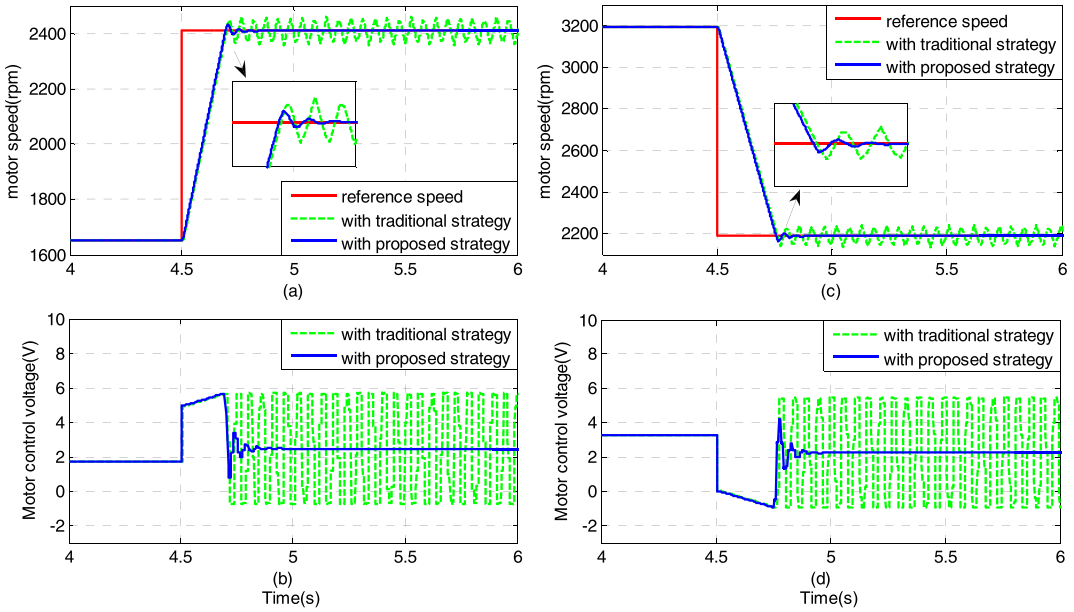

FIGURE 10. Simulation results in MIL simulation tests. (a–b) The speed synchronization in the downshift process. (c–d) The speed synchronization in the upshift process.

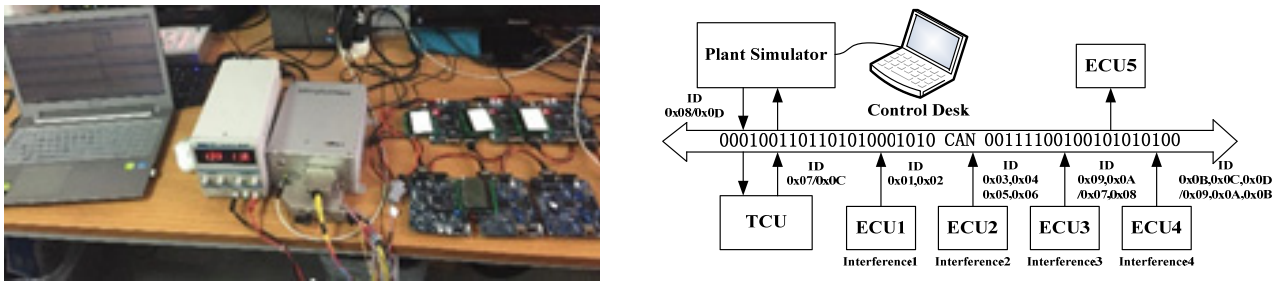

FIGURE 11. HIL experiment platform.

Figure 8 shows the IMT powertrain system diagram with network model, where a CAN is realized using a high-fidelity model of the TrueTime network block. The MAC protocol is specified as CSMA/AMP (CAN). The speed signal is feedback to TCU node by CAN and the command signal is sent to MCU node by CAN as well. The network parameters and all message packages and their priorities are set as in to Table 1 and Table 2 respectively.

Figure 9 shows the network transmission status of these messages with two different methods. As shown in Figure (a), with the proposed method, the network-induced delay of the ''Motor speed'' in each period is described by the total width consisting of a secondary-high level and a high level in the Line 1 (the secondary-high level denotes the queuing delay as in the expression (7) and the high level denotes the physical transmission time as in the expression (8)). Similarly, the network-induced delay of the ''Control signal'' in each period is described by the total width of a secondary-high level and a high level in the Line 2 in the Figure 9(a). Correspondingly, with the traditional method, the network-induced delays of the ''Motor speed'' signal and the ''Control signal'' are shown in the Line 1 and the line 2 of Figure 9(b), respectively.

The results show that, compared to the traditional method, the proposed method can obviously reduce the network-induced delays of the ''Motor speed'' and the ''Control signal''. As shown in Table 1, with the proposed method the maximum delay in the loop is 5.108 *ms*, whereas with the traditional method the maximum delay in the loop is 8.308 *ms*. Compared to the traditional method, the proposed method reduces the delay by 38.517%.

Figure10 shows the test results of the speed synchronization response in the MIL simulations. With the traditional method, significant oscillations with the amplitude of around 90rpm occur in the speed synchronization in both two shifting processes. Meanwhile, the severe chattering phenomenon of the motor control voltage is also caused in two shifting processes. However, with the proposed method, the speed synchronization response is still satisfactory. No speed tracking error occurs in the steady phase and the response time is around 0.30s in the downshift process and 0.34s in the

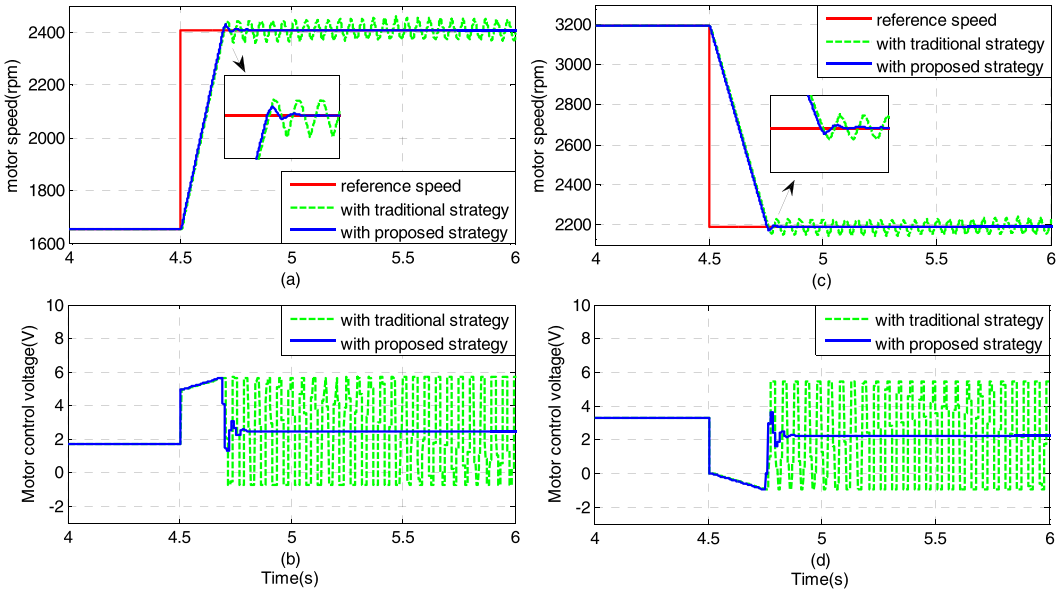

FIGURE 12. Test results in HIL experiments. (a–b) The speed synchronization in the downshift process. (c–d) The speed synchronization in the upshift process.

upshift process, respectively. Meanwhile, the slight chattering of motor control voltage only occurs in the transient phase, which is still satisfactory.

The results in the MIL tests show that the proposed method is more robust than the traditional method which is designed without considering the effects of the CAN system in the speed synchronization process.

V. HARDWARE-IN-LOOP EXPERIMENT

To validate the proposed method in a real CAN environment, hardware-in-loop (HIL) tests are implemented in this section. The HIL test system consisting of a dSPACE MicroAutoBox simulator and six 16-bit MC9S12XF512 based ECUs which are linked by a CAN is set up as shown in Figure 11.

In the HIL test, the IMT powertrain model is loaded into the MicroAutoBox simulator, which is a real-time digital system based on a DS1401 board. In the IMT powertrain model, there are two logical CAN nodes: the motor sensor node and the motor actuator node. The motor sensor node samples the motor signal and sends it to TCU node via CAN and the motor actuator node receives the command signal from the TCU node via CAN and executes it. The two nodes are connected to CAN by a CAN interface of the MicroAutoBox simulator as shown in Figure.11. Meanwhile, one ECU is chosen as the TCU node, which receives the motor speed signal, calculates the control command and sends the command signal in event-driven mode to the motor actuator node by the CAN. Another ECU is used to collect data for result analysis as ECU5 in Figure 11. The remaining 4 ECUs respectively denotes 4 control units for other functions which are connected into the CAN (called the interference nodes). They respectively send different interference messages with different IDs periodically shown in Table 2. The parameters of the real CAN system are chosen as same as those in simulations according to Table 1. Moreover, nodes and messages are also defined according to Table 2. In the HIL tests, the messages are practically exchanged among these nodes as shown in Figure 11.

Figure 12 shows the test results of the speed synchronization in HIL experiences. These results of HIL tests are almost similar with previous MIL simulations. With the traditional controller, the significant oscillations occur in the speed synchronization in two shifting processes and the severe chattering phenomenon of the motor control voltage is also caused in two shifting processes. However, the proposed controller demonstrates good robustness against the network-induced delays caused by CAN.

Therefore, the proposed method based on the co-design methodology of scheduling and control can effectively deal with the effects of network-induced delays caused by CAN and at the same time ensure the stability of the speed synchronization for clutchless IMT powertrain system.

In addition, the motor control voltage signal in the real CAN system is slightly smoother than that in MIL simulation, which is owing to the worst-case padding bits in CAN data frames considered in the simulation.

VI. CONCLUSIONS

In order to improve the speed synchronization performance in shifting process for the clutchless IMT powertrains using CAN, not only the network-induced delay but also the protocol constraints such as the packet capability and utilization ratio limitation should be considered. In this study, the network-induced delay model considering the packet capability and utilization ratio limitation is derived. The co-design procedure is presented based on Lyapunov stability theory and offline priority scheduling. The results of co-simulations

TABLE 1. System parameters.

Symbol	Description	Value/Unit
i_1	1th speed radio	1.75
i_2	2nd speed radio	1.2
i_g	Main reducer radio	4.1
$\Delta\omega_{1\to2}$	Motor speed range in upshift	3192-2189/rpm
$\Delta\omega_{2\to1}$	Motor speed range in downshift	1652-2409/rpm
R	Baud rate in CAN network	250/Kbit/s
d_j	Data size in the jth message packet	8/bytes
$\overline{\tau}_{\max}$	Upper bound of the delay	7.5/ms
$\tau_{\max,1}$	Max delay before scheduling	8.308/ms
$\tau_{\max,2}$	Max delay after scheduling	5.108/ms

TABLE 2. Communication protocol definition.

Nodes	Cycle/ Package number	priority	
		Before scheduling	After scheduling
Interference node 1	10ms /2	1,2	1,2
Interference node 2	10ms /4	3,4,5,6	3,4,5,6
Interference node 3	10ms /2	7,8	9,10
Interference node 4	10ms /3	9,10,11	11,12,13
Speed sensor	10ms /1	13	8
Control signal	Event trigger	12	7
The worst-case delay $\tau'_{\max}$		8.308/ms	5.108/ms

and HIL tests in upshift and downshift processes show that the proposed method can effectively deal with the effects of the CAN and ensure the stability of speed synchronization control. The comparison results also illustrate the co-design method has obvious advantages over the traditional method.

APPENDIX

See Table 1 and 2.

REFERENCES

[1] X. Zhu, H. Zhang, B. Yang, and G. Zhang, "Cloud-based shaft torque estimation for electric vehicle equipped with integrated motor-transmission system," *Mech. Syst. Signal Process.*, vol. 99, pp. 647–660, Jan. 2017.
[2] H. He, Z. Liu, L. Zhu, and X. Liu, "Dynamic coordinated shifting control of automated mechanical transmissions without a clutch in a plug-in hybrid electric vehicle," *Energies*, vol. 5, pp. 3094–3109, Aug. 2012.
[3] H. Liu, Y. Lei, Z. Li, J. Zhang, and Y. Li, "Gear-shift strategy for a clutchless automated manual transmission in battery electric vehicles," *SAE Int. J. Commercial Vehicles*, vol. 5, no. 1, pp. 57–62, 2012.
[4] H. Fu, G. Tian, Q. Chen, and Y. Jin, "Hybrid automata of an integrated motor-transmission powertrain for automatic gear shift," in *Proc. Amer. Control Conf.*, San Francisco, CA, USA, Jun./Jul. 2011, pp. 4604–4609.
[5] X. Dong and J. Xi, "The study of shift strategy for pure electric bus without synchronizer," in *Proc. Int. Conf. Electron. Mech. Eng. Inf. Technol.*, Aug. 2011, pp. 2557–2562.
[6] Y.-S. Yoon, S. J. Kim, and K.-S. Kim, "Conceptual design of economic hybrid vehicle system using clutchless geared smart transmission," *Int. J. Automotive Technol.*, vol. 14, no. 5, pp. 779–784, 2013.
[7] C.-Y. Tseng and C.-H.Yu, "Advanced shifting control of synchronizer mechanisms for clutchless automatic manual transmission in an electric vehicle," *Mech. Mach. Theory*, vol. 84, pp. 37–56, Feb. 2015.
[8] X. Zhu, H. Zhang, and Z. Fang, "Speed synchronization control for integrated automotive motor–transmission powertrain system with random delays," *Mech. Syst. Signal Process.*, vols. 64–65, pp. 46–57, Dec. 2015.
[9] C.-H. Yu and C.-Y. Tseng, "Research on gear-change control technology for the clutchless automatic–manual transmission of an electric vehicle," in *Proc. Inst. Mech. Eng. D, J. Automobile Eng.*, vol. 227, no. 10, pp. 1446–1458, 2013.
[10] C.-H. Yu, C.-Y. Tseng, and C.-P. Wang, "Smooth gear-change control for EV clutchless automatic manual transmission," in *Proc. IEEE/ASME Int. Conf. Adv. Intell. Mechatronics*, Jul. 2012, pp. 971–976.
[11] X. Zhu, H. Zhang, J. Xi, J. Wang, and Z. Fang, "Robust speed synchronization control for clutchless automated manual transmission systems in electric vehicles," *Proc. Inst. Mech. Eng. D, J. Automobile Eng.*, vol. 229, no. 4, pp. 424–463, 2014.
[12] S. Shaohua, L. Yulong, Y. Cheng, and W. Jietao, "Analysis and control of shift process for AMT without synchronizer in battery electric bus," presented at the 2nd Int. Conf. Electron. Mech. Eng. Inf. Technol. (EMEIT), 2012, pp. 1–6.
[13] G. Cusimano and F. Casolo, "An almost comprehensive approach for the choice of motor and transmission in mechatronics applications: Motor thermal problem," *Mechatronics*, vol. 40, pp. 96–105, Dec. 2016.
[14] G. Cusimano, "Choice of motor and transmission in mechatronic applications: Non-rectangular dynamic range of the drive system," *Mech. Mach. Theory*, vol. 85, pp. 35–52, Mar. 2015.
[15] D.-T. Qin, M.-Y. Yao, S.-J. Chen, and S.-K. Lyu, "Shifting process control for two-speed automated mechanical transmission of pure electric vehicles," *Int. J. Precis. Eng. Manuf.*, vol. 17, no. 5, pp. 623–629, May 2016.
[16] Z. Zhong, G. Kong, Z. Yu, X. Xin, and X. Chen, "Shifting control of an automated mechanical transmission without using the clutch," *Int. J. Automotive Technol.*, vol. 13, no. 3, pp. 487–496, 2012.
[17] W. Cao, H. Liu, C. Lin, Y. Chang, Z. Liu, and A. Szumanowski, "Speed synchronization control of integrated motor–transmission powertrain over CAN through active period-scheduling approach," *Energies*, vol. 10, no. 11, p. 1831, 2017.
[18] W. Cao, H. Liu, C. Lin, Y. Chang, Z. Liu, and A. Szumanowski, "Co-design based lateral motion control of all-wheel-independent-drive electric vehicles with network congestion," *Energies*, vol. 10, no. 10, p. 1641, 2017.
[19] W. Cao, Z. Liu, Y. Chang, and A. Szumanowski, "Direct yaw-moment control of all-wheel-independent-drive electric vehicles with network-induced delays through parameter-dependent fuzzy SMC approach," *Math. Problems Eng.*, vol. 2017, Jan. 2017, Art. no. 5170492.
[20] C. F. Caruntu, M. Lazar, R. H. Gielen, P. P. J. van den Bosch, and S. Di Cairano, "Lyapunov based predictive control of vehicle drivetrains over CAN," *Control Eng. Pract.*, vol. 21, no. 2, pp. 1884–1898, Dec. 2013.
[21] X. Zhu, H. Zhang, D. Cao, and Z. Fang, "Robust control of integrated motor-transmission powertrain system over controller area network for automotive applications," *Mech. Syst. Signal Process.*, vols. 58–59, pp. 15–28, Jun. 2015.
[22] X. Cao, P. Cheng, J. Chen, and Y. Sun, "An online optimization approach for control and communication codesign in networked cyber-physical systems," *IEEE Trans Ind. Informat.*, vol. 9, no. 1, pp. 439–450, Feb. 2013.
[23] S.-L. Dai, H. Lin, and S. S. Ge, "Scheduling-and-control codesign for a collection of networked control systems with uncertain delays," *IEEE Trans. Control Syst. Technol.*, vol. 18, no. 1, pp. 66–78, Jan. 2010.
[24] H. Xu, A. Sahoo, and S. Jagannathan, "Stochastic adaptive event-triggered control and network scheduling protocol co-design for distributed networked systems," *IET Control Theory Appl.*, vol. 8, no. 18, pp. 2253–2265, 2014.
[25] L. Zhang, Y. Shi, T. Chen, and B. Huang, "A new method for stabilization of networked control systems with random delays," *IEEE Trans. Autom. Control*, vol. 50, no. 8, pp. 1177–1181, Aug. 2005.
[26] C. F. Caruntu and C. Lazar, "Network delay predictive compensation based on time-delay modelling as disturbance," *Int. J. Control*, vol. 87, no. 10, pp. 2012–2026, 2014.
[27] H. Chen, X. Cheng, and G. Tian, "Modeling and analysis of gear-shifting process of motor-transmission coupled drive system," *J. Comput. Nonlinear Dyn.*, vol. 11, no. 23, p. 021013, Jan. 2016.
[28] Y. Shi and B. Yu, "Robust mixed H_2/H_∞ control of networked control systems with random time delays in both forward and backward communication links," *Automatica*, vol. 47, no. 4, pp. 754–760, Apr. 2011.

[29] T. Nolte, H. Hansson, and C. Norstrom, "Probabilistic worst-case response-time analysis for the controller area network," in *Proc. 9th IEEE Real-Time Embedded Technol. Appl. Symp.*, May 2003, pp. 200–207.
[30] K. Tindell, A. Burns, and A. J. Wellings, "Calculating controller area network (can) message response times," *Control Eng. Pract.*, vol. 3, no. 8, pp. 1163–1169, Aug. 1995.

WANKE CAO received the B.E. degree in mechanical engineering and automation and the Ph.D. degree in vehicle engineering from Northeastern University, Shenyang, China, in 2003 and 2008, respectively. From 2008 to 2010, he was a Post-Doctoral Researcher with the Department of Vehicle Engineering, Beijing Institute of Technology (BIT), Beijing, China. He was a Visiting Scholar with the Department of Multisource Propulsion Systems, Warsaw University of Technology, Warsaw, Poland, from 2015 to 2016. He is currently a Lecturer with the National Engineering Laboratory for Electric Vehicles and the Collaborative Innovation Center of Electric Vehicles in Beijing, School of Mechanical Engineering, BIT. His current research interests include networked control of electric vehicles, vehicle dynamics and control, fuzzy control, sliding mode control, and the in-vehicle network technology.

YINGSHUANG WU received the B.E. degree in mechanical engineering and automation from Chang'an University, Xi'an, China, in 2017. She is currently pursuing the master's degree with the Department of Vehicle Engineering, Beijing Institute of Technology. Her current research interests include networked control technologies of electric vehicles and the in-vehicle network technology. She received the National Scholarship for two years.

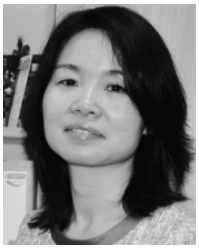

YUHUA CHANG received the M.Sc. and Ph.D. degrees from the Warsaw University of Technology (WUT) in 2005 and 2007, respectively. Since 2003, she has been a Researcher in battery modeling and management for E&HEVs, and the configuration design of the propulsion system for HEVs by simulation. She has been involved in several Polish national and EU projects regarding the technologies of E&HEVs, electromobility, and green transportation. She is currently an Adjunct Professor with the Department of Multisource Propulsion System, WUT.

ZHIYIN LIU received the M.Sc. and Ph.D. degrees from the Warsaw University of Technology (WUT) in 2008 and 2015, respectively. Since 2009, he has been a Researcher in HEVs and EVs propulsion system simulation and their components design. He is currently an Adjunct Professor with the Department of Multisource Propulsion System, WUT.

CHENG LIN is currently a Professor with the Beijing Institute of Technology. Since 2002, he has been a Researcher in EVs. His current research interests include motion control and integration technologies of electric vehicle.

QIANG SONG received the Ph.D. degree from the Beijing Institute of Technology (BIT) in 2004. He is currently an Associate Professor with BIT. Since 2004, he has been a researcher in electric motor propulsion system. His current research interests include electric motor testing, driving, and control technologies.

ANTONI SZUMANOWSKI received the Ph.D. and D.Sc. degrees from the Warsaw University of Technology (WUT), Poland. He is currently a Professor at WUT and the Head of the Department of Multisource Propulsion Systems. He has authored over eight books (five in Polish and three in English) in the field of electric and hybrid electric vehicles (E & HEVs), alternative energy, and energy storage system He has been involved in E & HEVs research since 1976 and many Polish national and EU projects in the fields of E & HEVs, electromobility, and green transportation.